Molecular Crystals and Liquid Crystals

Publication details, including instructions for authors and subscription information:
http://www.tandfonline.com/loi/gmcl20

Mechanical Properties of Freely Suspended LC Filaments

Alexandru Nemeş [a], Alexey Eremin [a] & Ralf Stannarius [a]

[a] University of Magdeburg, Institute of Experimental Physics, Universitätsplatz, Magdeburg, Germany

Version of record first published: 31 Aug 2006

To cite this article: Alexandru Nemeş, Alexey Eremin & Ralf Stannarius (2006): Mechanical Properties of Freely Suspended LC Filaments, Molecular Crystals and Liquid Crystals, 449:1, 179-189

To link to this article: http://dx.doi.org/10.1080/15421400600584495

Mol. Cryst. Liq. Cryst., Vol. 449, pp. 179–189, 2006

ISSN: 1542-1406 print/1563-5287 online
DOI: 10.1080/15421400600584495

Mechanical Properties of Freely Suspended LC Filaments

Alexandru Nemeş
Alexey Eremin
Ralf Stannarius
University of Magdeburg, Institute of Experimental Physics, Universitätsplatz, Magdeburg, Germany

In several mesophases of bent-core liquid crystals, stable freely suspended filaments can be prepared. In this paper, we report a study of smectic liquid-crystal filaments formed by bent-shaped molecules in different mesophases, focused on a mechanical and structural characterization of the filaments.

Keywords: bent-core mesophases; free standing filaments; structure characterization

INTRODUCTION

Bent-core molecules have not only peculiar chirality and polarity properties, but also striking rheological and structural features, such as the formation of stable free-standing liquid filaments. In our work, we study free-standing filaments of few micrometers thickness and lengths of several millimeters drawn in several mesophases (Table I, Fig. 1) with focus on understanding of the filaments structure, their stability and mechanical properties.

All mesogens except of compound **4** exhibit polar smectic C (SmCP) phases. In these phases, the molecules are tilted with respect to the layer plane and the spontaneous polarization vector is perpendicular to the layer normal. Some possible modifications lead to the existence of polymorphic variants of the SmCP phase [1]. A higher ordered

The authors acknowledge support by the DFG within grant STA-425/15. H. Nádasi and W. Weissflog are gratefully acknowledged for supply of the mesogenic material. The authors also thank M. Schulz for X-Ray measurements, I. Grodrian and L. Naji for AFM data.

Address correspondence to Alexandru Nemeş, University of Magdeburg, Institute of Experimental Physics, Universitätsplatz 2, D-39106, Magdeburg, Germany. E-mail: alexandru.nemes@physik.unl-magdeburg.de

TABLE I Investigated Compounds and Phase Behavior

Name	R	X	Y	n	Phase behavior and transition temperatures (°C)					
1	H	F	–N=CH–	10	**I**	160	**SmX**	143	**SmCP**	90	**S**
2	5-F	F	–N=CH–	9	**I**	154	**SmCP**	130	$\mathbf{B_5}$	99	**S**
3	2-CH_3	F	–N=CH–	11	**I**	153	**SmCP**	114	$\mathbf{B_5}$	100	**S**
4	2-NO_2	H	–N=CH–	16	**I**	172	$\mathbf{B_7}$	101		**S**	

phase, with an additional in-plane order, is called B_5 (compounds **2**, **3**). The so far not unambiguously classified SmX phase has a layer structure and many features in common with the B_7 phase [2]. The structure of the investigated bent-core mesogenic materials is presented in the Figure 1 below.

One of the main characteristics of fluid filaments is their length to diameter ratio, the so-called slenderness ratio. The filaments formed by banana phases are known to have a particularly high slenderness ratio above 1000 [3,4]. It is much higher than the slenderness ratio of smectic A filaments (4.2 in microgravity) and even higher than in the columnar phases of disk-shaped molecules (>100) [5].

In polymeric nematics and columnar phases, strain hardening leads to the formation of fibers. However, in the case of bent-core mesogens, the stability of liquid filaments is provided by the molecular layer structure of the smectic mesophases, e.g., when the layers are wrapped cylindrically around an axial core.

Filaments could be drawn in the SmX and SmCP, B_5 and B_7 phases. Their appearance and stability depends very much on the phases and materials. Filaments in the B_7 phase of compound **4** are quite thin (less than 20 μm), they could be kept for several days in the laboratory, so that we expect that they are stable and their lifetime is practically unlimited. The same applies to the filaments in the SmX phase of

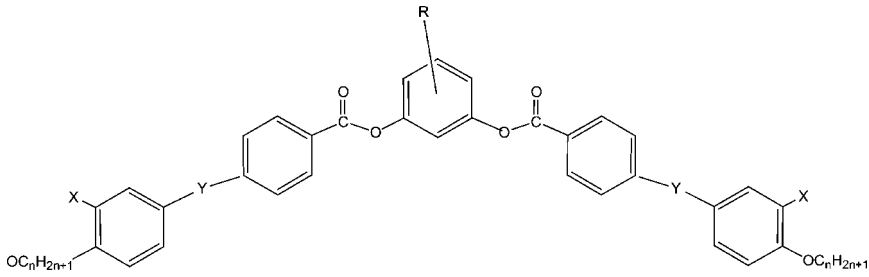

FIGURE 1 Chemical composition of the investigated materials.

compound **1**, the lifetime is practically unlimited but the filaments are usually in the thickness range up to 100 μm. In the SmCP phase of the same material, filaments broke after few hours, probably they are sensitive to slight mechanical disturbances. In the compound **3**, no filaments could be drawn in B_5, and filaments in the SmCP phase proved to be stable only for few seconds. Finally, in compound **2**, filaments could be drawn in the B_5 and SmCP phases but their lifetime in SmCP was generally restricted to a few minutes.

EXPERIMENT

The filaments are prepared in different mesophases as presented in Table 1. It is established from X-Ray measurements that the filaments are composed of smectic layers cylindrically wrapped around one or more axial cores (Fig. 2). They represent either single cylindrical fibrils or bundles of fibrils with diameters from few micrometers to approximately 100 μm. Filaments are pulled with a needle at a constant speed (less then 1 mm/s) from the bulk material. They retain a uniform diameter during the pulling process; new material is constantly supplied form the meniscus.

In order to measure the static filament tension, the following experiment was performed: the filament was drawn with a cantilever, consisting of a 8 layers of 5 μm thick gold plates with a small tip near the cantilever end. The filament tension was determined from the deflection of the cantilever. The measurements in this experiment

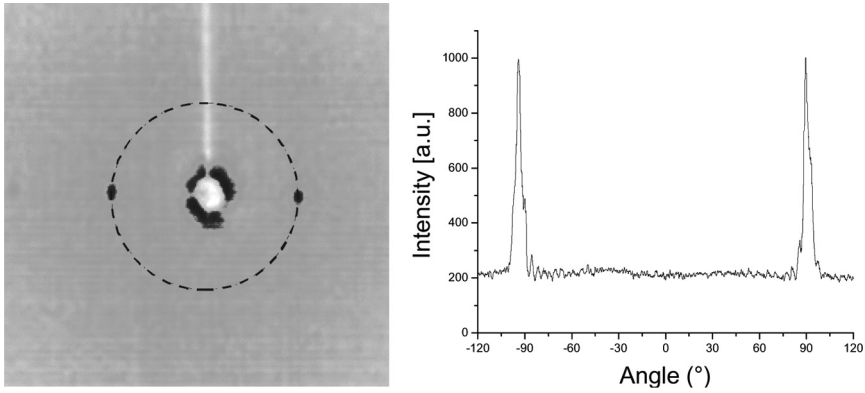

FIGURE 2 (a) Two-dimensional X-Ray pattern of a free-standing filament (the scattering vector is perpendicular to the fiber). (b) Intensity distribution as function of scattering azimuth at fixed scattering angle (dashed line in (a)).

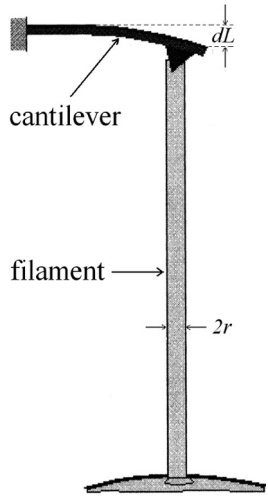

FIGURE 3 Setup for measurements of the filament tension. Filament and cantilever are enclosed in a temperature controller box. We observe the cantilever deflection with a long range microscope.

were done in the SmX phase at T = 155°C (compound **1**). The principal geometry of this experiment is depicted in Figure 3.

In a second experiment, dynamic properties of filaments have been studied. The filament is deflected form its initial equilibrium shape by means of an electric field, and the relaxation behavior is recorded after the electric field was switched off. Filaments were drawn in the B_7, SmX or SmCP phases. The geometry of this experiment is shown in Figure 4.

In both experiments, the setup is enclosed in a copper heating box for temperature stability and protection against air flow. Temperature is controlled with an accuracy of 1 K. The box has two quartz windows for optical observation. We illuminate the filaments with parallel monochromatic light. The observation axis is perpendicular to the filament axis. The optical transmission images are recorded either with a Nikon Coolpix 990 digital photo camera (stationary images) or with a high speed Citius Imaging C10 video camera (dynamic measurements) mounted on a Questar QM 100 long range microscope.

RESULTS AND CONCLUSIONS

The first mechanical experiment was set up to measure the static tension, which is expected to reflect the surface tension of the material respective to air. The cantilever deflection as a function of the force

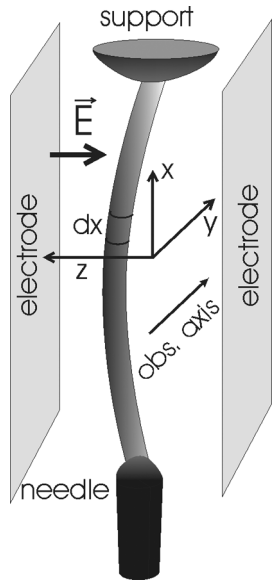

FIGURE 4 Schematic setup for the preparation and electrical deflection of liquid filaments. The complete setup is contained in a heating box with glass observation windows, the filament is observed by means of a long range microscope.

exerted to the tip has been gauged. The force constant, given by the product of Young modulus and geometrical inertia moment of the cantilever cross section was measured (around 4.6 μN). Thin filaments were drawn and the deflection of the cantilever, dL has been measured (see Fig. 3).

Assuming that the filaments have a perfectly cylindrical form, the surface energy E_s can be expressed by the radius r, length L and surface tension σ as $E_s = 2\pi rL\sigma$. This formula allows to estimate the surface tension from the measured stress $\mathrm{d}E_s/\mathrm{d}L$. The surface tension measured in case of different radii at the temperature $\mathrm{T} = 155^{\circ}\mathrm{C}$ gave a value of $\sigma = 26 \pm 2\,\mathrm{mN/m}$ under the assumption of a smooth, cylindrical surface. In fact, as seen in AFM images (Fig. 5), the surface of filaments is corrugated and if one takes into account that the actual filament surface is higher than that of a smooth cylinder of same radius, this value for σ is probably overestimated by 20–30%. The measured tension of the filaments complies with the values of the surface tension in conventional smectics. These results corroborate our assumption of compact filament structure where surface tension plays a dominant role.

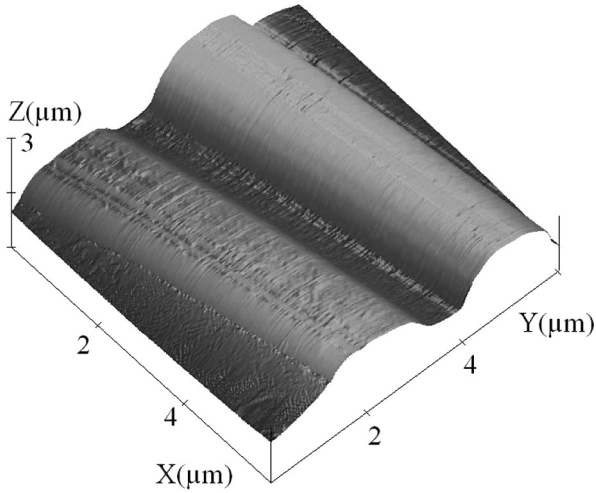

FIGURE 5 AFM height profile of a typical filament with 50 μm diameter. The surface undulations are parallel to the fiber axis.

In absence of external forces, the filaments adopt a perfectly straight shape. Application of a strong external DC electric field perpendicular to the axis of the filament leads to a lateral deflection. The bend deformation consists essentially of the ground mode $z(x) = z_0 \cos(kx)$ with $k = \pi/L$. The deflection is independent of the sign of the electric field, but in the plane of electric field and initial (vertical) filament axis (see Fig. 4). Upon switching the polarity of the electric field, the filaments usually deflect in the same direction, with the same amplitude. The deflection exhibits a threshold-like behaviour and the amplitude of the deflection z_0 increased with the decreasing of the filament radius and with the increasing of the filament length or with the increasing of external electric field strength. The latter is chosen between 100 and 700 V/mm, so that the deflection amplitude z_0 is a few percent of the filament length (Fig. 6)

The typical dynamics of the deflection is shown in Figure 7 for a filament with length $L = 2.96$ mm and radius $r = 25$ μm, that has been draw in the SmX phase (T = 150°C, compound 1) after an electric field of 330 V/mm has been switched on at t = 0.3 s and off at $t_0 = 3.2$ s. The deformation is a two step process, an immediate, fast initial response, which is probably driven by dielectric interactions, followed by a slow deflection with much larger amplitude, which is attributed to a gradual charging of the filament by ion transport in the electric field, until the filament forms an equipotential line.

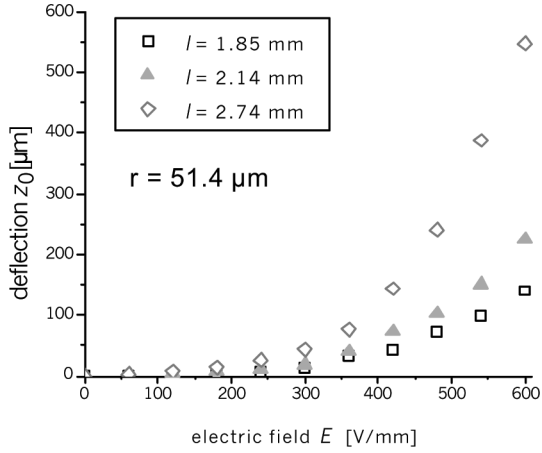

FIGURE 6 Maximum deflection z_0 as a function of the applied electric field strength measured in the middle of the filament for different lengths (SmX, compound **1**).

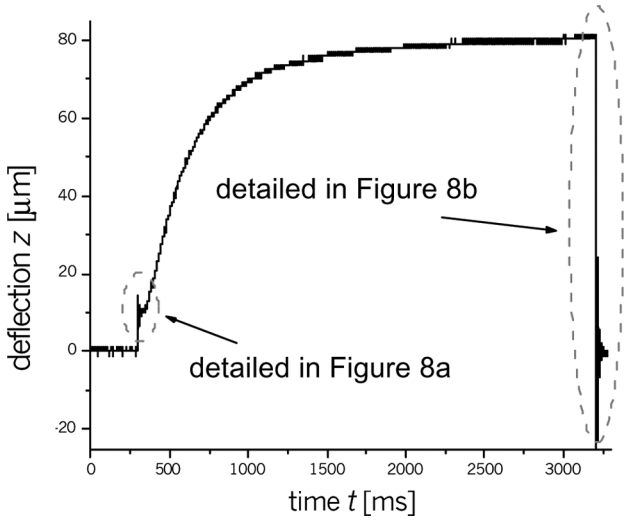

FIGURE 7 Typical dynamics of the deflection amplitude (compound **1**, SmX at 150°C), the field is switched on after 0.3 s and off after 3.2 s. Details are shown in Figures 8a and 8b.

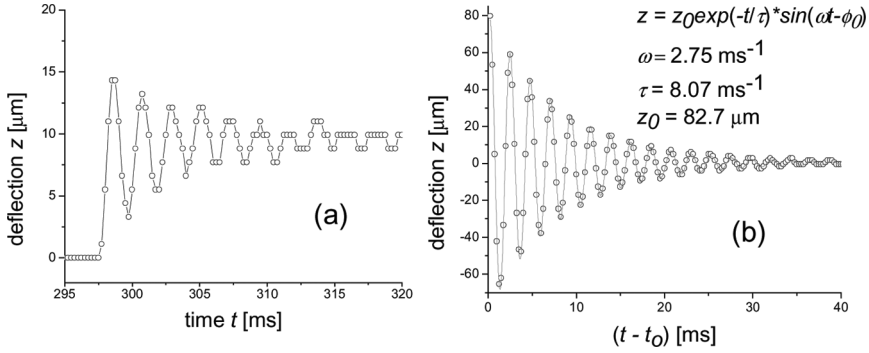

FIGURE 8 (a) Details of the oscillation immediately after the electric field has been switched on. (b) Damped oscillation towards the straight ground state after the electric field has been switched off. Solid line is a fit with $z = z_0 \exp(-t/\tau) \sin(\omega t - \psi_0)$.

The measurements performed with different filaments in the SmX phase of compound **1** show that the dynamics of the damped oscillations does not depend on the strength and polarity of the electric field applied for the initiation of the deflection (Fig. 9). So, in case of the free oscillations, the nature of the electric forces is not relevant, it will be investigated in detail in forthcoming work.

Measurements of the oscillation parameters in the SmX phase and in the SmCP phase of compound **1** showed similar results: a linear dispersion relation $\omega(k)$. This result corresponds to a dispersion free wave velocity $c = \omega/k$ of approximately 2.6 m/s (Fig. 10).

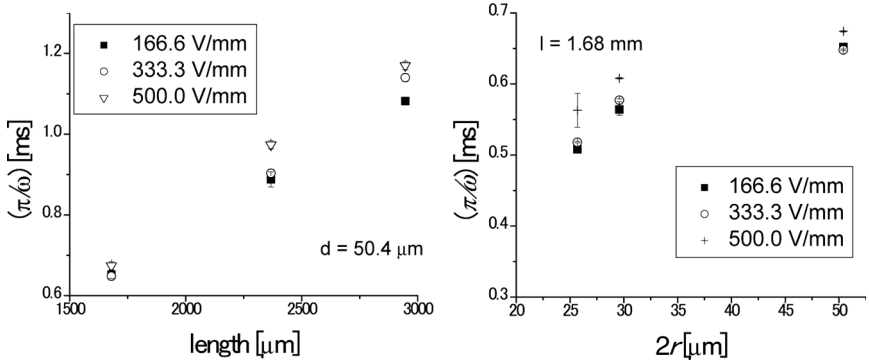

FIGURE 9 Independence of the oscillation frequency ω of the damped oscillations on the initial electric field strength.

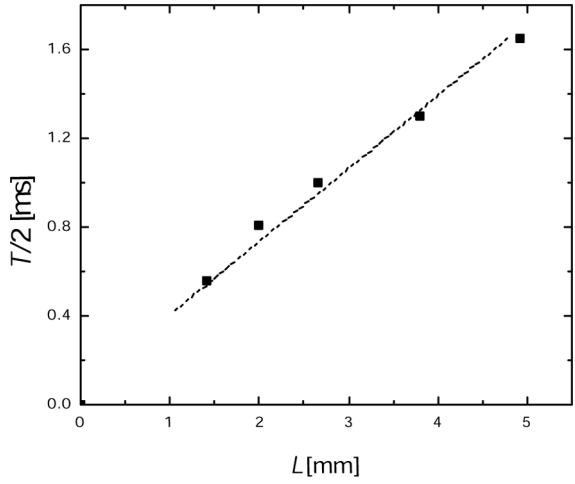

FIGURE 10 Linear dependence of the oscillation period T on the filament length L.

The temperature dependence of the oscillations has been recorded in the SmX and SmCP phases of compound **1** across a range of about 40 K. Fourier transforms of the free oscillations as a function of temperature (power spectral densities) are shown in Figure 11. The oscillation frequency decreases with increasing temperature. On

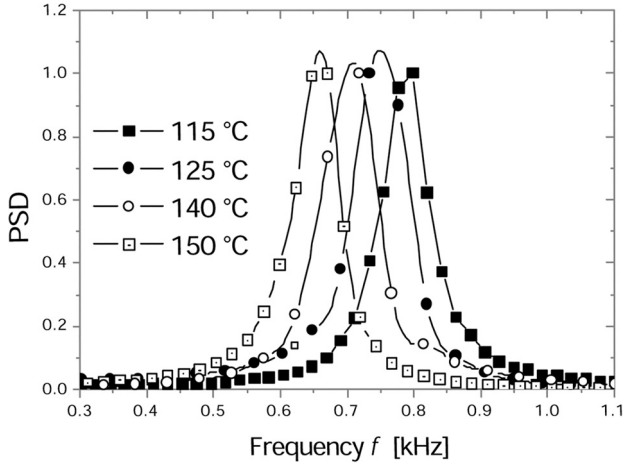

FIGURE 11 Temperature dependence of the oscillation. The graphs show the power spectral densities at four selected temperatures.

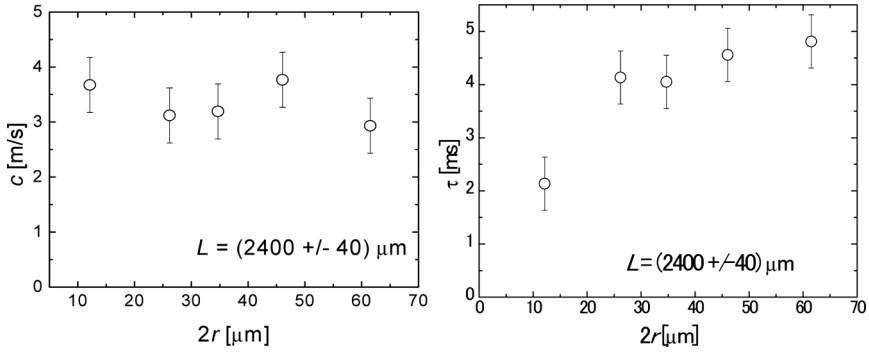

FIGURE 12 Dependence of the wave velocity $c = \omega/k$ and damping time τ on the filament radius r. Measurements have been performed on several filaments with approximately the same lengths.

the other hand, there is practically no temperature dependence of the decay rate of the oscillations (reflected in the half width of the resonance curves).

The dependence of resonance frequency and damping rates on the filament radius has been measured in a range between 6 and 30 μm. The oscillation frequency proves to be practically radius independent; the damping constant shows a weak systematic decrease at small radii (Fig. 12).

The measured dynamics can be sufficiently explained by a simple harmonic oscillator model. An equation of motion of the liquid

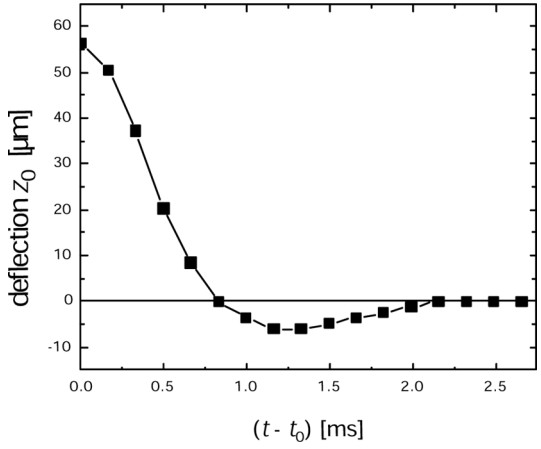

FIGURE 13 Typical relaxation of a filament in the B_7 phase.

filaments can be constructed from inertial, elastic, surface tension and friction terms that influence the dynamics of vibrations in absence of external forces. Details of the calculations are given in [6].

Finally, it is observed that the same experiments performed with filaments pulled in the B_7 mesophase of compound **4** yields a qualitatively different picture, no damped oscillations are found there, but a strongly damped relaxation (Fig. 13) which does not allow to determine the oscillation frequency from the experimental data.

REFERENCES

[1] Eremin, A., Wirth, I., Diele, S., Pelzl, G., Schmalfuss, H., Kresse, H., Nádasi, H., Fodor-Csorba, K., Gacs-Baitz, E., & Weissflog, W. (2002). *Liq. Cryst.*, *29*, 775.
[2] Eremin, A., Diele, S., Pelzl, G., Nádasi, H., & Weissflog, W. (2003). *Phys. Rev. E*, *67*, 021702.
[3] Jakli, A., Krüerke, D., & Nair, G. G. (2003). *Phys. Rev. E*, *67*, 051702.
[4] Eremin, A., Nemes, A., Stannarius, R., Schulz, M., Nádasi, H., & Weissflog, W. (2005). *Phys. Rev. E*, *71*, 031705.
[5] van Winkle, D. H. & Clark, N. A. (1982). *Phys. Rev. Lett.*, *48*, 1407; Mahajan, M. P., Tsige, M., Taylor, P. L., & Rosenblatt, C. (1996). *Liq. Cryst.*, *26*, 443.
[6] Stannarius, R., Nemes, A., & Eremin, A. *Phys. Rev. E*, *72*, 020702(R).